Structure of Poly(vinyl alcohol) Cryo-Hydrogels as Studied by Proton Low-Field NMR Spectroscopy

J. L. Valentín,*,†,‡ D. López,‡ R. Hernández,‡ C. Mijangos,‡ and K. Saalwächter†

Martin-Luther-Universität Halle-Wittenberg, Institut für Physik, Betty-Heimann-Str. 7, D-06120 Halle, Germany, and Institute of Polymer Science and Technology (CSIC), C/Juan de la Cierva 3, 28006 Madrid, Spain

Received September 24, 2008; Revised Manuscript Received November 13, 2008

ABSTRACT: The network structure of poly(vinyl alcohol) (PVA) hydrogels obtained by freezing−thawing cycles was investigated by solid-state ^{1}H low-field NMR spectroscopy. By the application of multiple-quantum NMR experiments, we obtain information about the segmental order parameter, which is directly related to the restrictions on chain motion (cross-links) formed upon gelation. These measurements indicate that the network mesh size as well as the relative amount of nonelastic defects (i.e., non-cross-linked chains, dangling chains, loops) decrease with the number of freezing−thawing cycles but are independent of the polymer concentration. The formation of the PVA network is accompanied by an increasing fraction of polymer with fast magnetization decay (∼20 μs). The quantitative study of this rigid phase with a specific refocusing pulse sequence shows that it is composed of a primary crystalline polymer phase (∼5%), which constitutes the main support of the network structure and determines the mesh size, and a secondary population of more imperfect crystallites, which increase the number of elastic chain segments in the polymer gel but do not affect the average network mesh size appreciably. Correspondingly, progressive melting of the secondary crystallites with increasing temperature does not affect the network mesh size but only the amount of network defects, and melting of the main PVA crystallites at ∼80 °C leads to the destruction of the network gel and the formation of an isotropic PVA solution.

Introduction

Poly(vinyl alcohol) (PVA) is a biocompatible polymer with a great variety of biomedical and pharmaceutical applications.[1−4] PVA in aqueous solution is able to form chemical or physical gels under a variety of conditions.[4−10]

The physical gelation capacity of PVA solutions has been well known for a long time;[11−13] however, the preparation of hydrogels by repeated freezing−thawing cycles has attracted renewed interest.[3,4,14−20] The high degree of swelling in water, the rubbery elasticity, the chemical and mechanical stability, the porous fibrilar network structure, and the lack of toxicity makes freeze−thaw PVA hydrogels an attractive polymer matrix for biotechnological applications.[14−20]

To understand the origin of these properties and therefore the bioapplicability of this material,[14−20] it is necessary to study the physical gelation process produced by the freezing−thawing cycles as well as the formed network structure.[21−23] Komatsu el al.[13] investigated the phase diagram of the water/PVA binary system. According to this diagram, gelation occurs with or without spinodal decomposition according to the polymer concentration and temperature. The process seems to start with a clustering of chains,[24,25] which is primarily caused by the association of polar groups of the dissolved polymer, followed by polymer crystallization. This means that the physical cross-links, which are responsible for the network formation, could be formed by different processes, such as hydrogen bonding, polymer crystallization, and in some cases (depending on the gelation conditions), phase separation.[14]

In addition, the application of freezing−thawing cycles to PVA solutions leads to the formation of heterogeneous networks with different morphology and properties as compared with nonfrozen gel systems. Peppas et al. were the pioneers in the development of this type of polymer cryogels.[7] In earlier work, they attribute the gel formation to a partial crystallization of chain segments to microcrystalline structures. X-ray diffraction studies[26,27] confirmed that polymer crystallites act as junction points. However, the intensity of the diffraction maximum that corresponds to the 101 reflection is clear for only PVA hydrogels with high polymer content.[13,27] For hydrogels with 10 to 15% polymer, solid-state NMR was used to identify and quantify the crystalline phase,[18,28] although X-ray analysis is also possible.[29]

Most recent works show that gelation by freeze−thaw processing forms heterogeneous networks of interconnected micro- and macropores. Willcox et al.,[28] in an exhaustive study using transmission electron microscopy (TEM) images and NMR, showed the formation of networks with rounded pore morphology, fibrillar network morphology, or both depending on the number of cycles as well as aging. They attribute the formation of cross-links to a kinetically frustrated crystallization in the first freezing cycle. After this process, subsequent cycles (or aging processes) lead to the creation of new (secondary) crystallites and the growing of the primary crystals; however, the mesh spacing slightly changes. This fact seems to indicate that the average distance between the primary crystallites that are formed during the first thermal treatment constitutes the main controlling factor for the network structure.

In addition, Auriemma and coworkers in a series of works[17,18,29−32] showed that the porous structure originates from freezing in the first step because of the incomplete crystallization of water. The polymer concentration in this unfrozen water phase is higher than that in the original solution, and the polymer network is formed within this microphase because of PVA crystallization. The cross-link points are therefore constituted of polymer crystallites, and the formed gels could be described by a bicontinuous structure of polymer-rich and polymer-poor regions. In contrast, Hernández et al.,[8−10] on the basis of DSC measurements, also inferred the possibility of the existence of covalent cross-links between the polymer chains brought about by the formation of radicals due to strong local shear during water crystal growth.[33]

* Corresponding author. E-mail: jlvalentin@ictp.csic.es.
† Martin-Luther-Universitat Halle-Wittenberg.
‡ Institute of Polymer Science and Technology (CSIC).

10.1021/ma802172g CCC: $40.75
Published on Web 12/12/2008

In summary, the PVA hydrogels obtained by freezing−thawing cycles appear to be constituted by a very complicated network structure that is based on different phenomena (i.e., crystallization, hydrogen bonding, liquid−liquid phase separation, and covalent bonds). Therefore, a complete analysis of this structure requires the use of different characterization techniques. However, most of them require the manipulation of the hydrogel sample, provoking changes in the original structure. For example, the use of chromatographic techniques or scattering techniques to measure molecular weight or cluster size requires the dilution of the gel[24] (although it was shown that it is possible). Mechanical measurements have the limitation of water evaporation at higher temperatures.[9] The cryo-TEM technique has the inconvenience of handling difficulties to avoid artifacts.[28] For the study of the crystallite content, very useful techniques such as differential scanning calorimetry (DSC) as well as X-ray diffraction are challenged by a sensitivity problem in dilute samples; for this reason, measurements were sometimes made in dry samples.[34] In this vein, solid-state NMR is a powerful tool for studying polymer networks,[35,36] but it has not been extensively used in this field.

The focus of this work is the use of a low-field NMR spectrometer to analyze the structure of the PVA gel in detail as a function of the freezing−thawing cycles, checking all of the structural models suggested in the literature. In addition, a melting process that transforms these physical gels into isotropic solutions of PVA in water was also studied. Importantly, we focus on detecting protons so that sensitivity, even at the low concentrations under study, is not a serious issue. The use of an inexpensive low-field NMR spectrometer on as-prepared samples to study this complex matrix has the advantage that several of the cited inconveniences in sample characterization are avoided. By using different NMR methodologies, we are able to carry out a complete and quantitative study of the complex structure exhibited by the PVA gels: multiple-quantum (MQ) NMR allows us to gain direct access to residual dipolar coupling constants that persist because of the existence of cross-links and other topological constrains.[38−40] Therefore, this experimental procedure is a powerful tool for quantifying the gelation process[41] and gives us quantitative detail on not only the microstructure[42] but also the dynamics[43] of the gel, that is, a complete picture of the network structure evolution depending on, for example, the number of freezing−thawing cycles. In addition, we used pulsed mixed magic-sandwich echo (MSE) experiments that provide a near-quantitative refocusing of the rigid contribution to the initial part of the free induction decay (FID)[44] and allow for an essentially quantitative determination of the crystallinity.

To our knowledge, this is the first time that advanced NMR pulse sequences performed on a low-field spectrometer were applied to the study of the network structure and phase composition of physical hydrogels.

Experimental Section

Materials and Sample Preparation. PVA was obtained from Aldrich. The sample was >99% hydrolyzed, had a weight-average molecular weight of 94 000 g/mol, and had syndio-, hetero-, and isotacticities of 17.2, 54.1, and 28.7%, respectively. PVA was dissolved in deuterated water (with polymer concentrations of 10 and 20% w/w) at 80 °C under continuous stirring to avoid inhomogeneities and local gelation. Solutions were stored at 80 °C overnight; then, they were cooled to room temperature for 1 h. Then, PVA solutions were introduced to 10 mm OD NMR tubes and were flame sealed to avoid variations in the water content. Two technical considerations are important at this point: (i) The quantity of sample inside the tube has to be ≲8 mm in height and located in the center of the radio frequency (rf) coil to ensure good rf field (B_1) homogeneity. (ii) The length of the NMR tube should be as short as possible for good control of the temperature. This is important because in this way, the whole tube can be inserted in the probe head, thus avoiding possible temperature gradients due to heat conduction.

PVA hydrogels were obtained by repetition of freezing−thawing cycles of solutions inside the sealed tubes that consisted of 1 h of cooling to −32 °C and 1 h of thawing at room temperature. After this process, samples were immediately inserted in the NMR spectrometer and measured to avoid the effect of aging. In some cases (specified below), the first freezing cycle was extended to ∼12 h (overnight), and subsequent cycles were 3 h long.

Description of Performed Solid-State Proton Nuclear Magnetic Resonance Experiments. Solid-state ^{1}H NMR spectroscopy is a powerful and widely used experimental technique in the field of polymer science.[35] In recent years, the use of inexpensive and easy-to-use low-field spectrometers[38,45,46] has gained the attraction of scientists because it certainly produces quantitative results on polymer structure and dynamics, albeit, of course, without chemical resolution. On the basis of different experiments, which will be extensively described in the next sections, applications include quantitative studies on polymer network structure[38] and polymer crystallization,[44] that is, the main topics of this study. In this work, experiments were carried out on a Bruker minispec mq20 spectrometer operating at 0.5 T with 90° pulses of 1.7 μs length and a dead time of 12 μs.

Proton Multiple-Quantum Nuclear Magnetic Resonance. MQ spectroscopy is one of the most versatile and robust quantitative techniques for investigating not only the structure but also the dynamics of polymer networks.[38] In solution, the fast segmental motion of the polymer chains through the different accessible conformations is isotropic and completely averages the dipolar coupling interaction that is typical for solid-state spectra. However, constraints, irrespective of their nature (e.g., cross-links, entanglements, or chain packing), lead to nonisotropic segmental fluctuations and therefore to the persistence of a weak residual dipolar coupling (D_{res}),[47−49] which is our central NMR observable. In other words, the measured effect relies on the orientation dependence of the fluctuating dipolar coupling tensor with respect to the magnetic field, which can be described by an orientation autocorrelation function of the individual chain segments. Fast segmental dynamics (in the range of nanoseconds to microseconds) lead to a loss of correlation to a plateau value that is related to the existence of preferential local orientation generated by the existence of cross-links. In fact, the measurable D_{res} is directly proportional to a local dynamic order parameter of the polymer backbone,[38] which is defined as a time average over the fluctuations of the segment-fixed dipolar tensor over the time until the plateau region is reached. It connects the experimental observable with the network parameters:

$$S_b = k\frac{D_{res}}{D_{stat}} = \frac{3}{5}\frac{r^2}{N} \quad (1)$$

Here D_{stat} is the segmental averaged dipolar coupling constant in the static limit and k is a rescaling factor that takes into account the fast dynamics (in the range of picoseconds) inside the statistical (Kuhn) segments. The NMR observable is related to r, that is, the ratio of the end-to-end vector to its average unperturbed melt state ($r^2 = \boldsymbol{r}^2/\langle \boldsymbol{r}^2\rangle_0$), and to N, the number of statistical segments between constraints.

A variety of NMR experiments[37,50−53] was used to detect residual dipolar couplings to monitor gelation processes, and recently, ^{1}H MQ NMR has evolved as the most powerful tool for obtaining a direct measurement of D_{res} and even its distribution.[38−40,54] Details of the pulse sequence as well as the data analysis are already published elsewhere.[38,41,55] Here we point out some relevant details of the current investigation.

Temperature usually plays an important role in MQ measurements[43] because as previously mentioned, the order parameter should be obtained as an average of the segmental fluctuations over all of the possible conformations on the experimental time scale (less than microseconds). Therefore, the temperature is required to

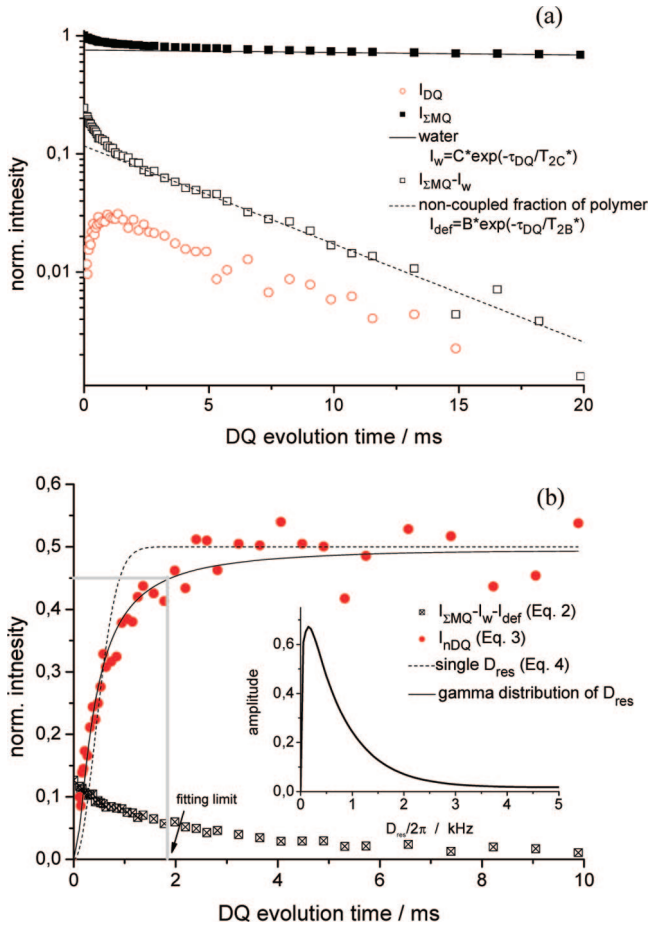

Figure 1. MQ NMR build-up and decay data for 10% PVA sample after one freezing−thawing cycle. (a) As-acquired I_{DQ} and $I_{\Sigma MQ}$ and (b) $I_{\Sigma MQ}$ (after extraction of noncoupled contributions) and normalized DQ build-up curves (I_{DQ}). The solid line in a represents the exponential fit for water subtraction, and the dashed line is the exponential fit representing the subtracted noncoupled polymeric defects. In b, solid and dashed lines represent the fits assuming a gamma distribution of D_{res} and a single residual dipolar constant, respectively. The insert is the result of a numerical analysis of I_{nDQ} via Tikhonov regularization.

be far above the polymer glass-transition temperature T_g to ensure that the segmental dynamics is fast enough to sweep out the whole conformational space between topological constraints and to achieve full averaging. If this is not the case, then the obtained D_{res} (and therefore the number of junctions in the network) will be overestimated.[41] In this work, the studied samples are hydrogels; therefore, the dissolved state of the polymer chain ensures that the segmental dynamics is indeed fast enough to detect the order parameter in the plateau regime, even at room temperature.

Similar to the traditional transverse relaxation experiments, the analyzed result of the MQ experiment is a time-dependent but normalized double-quantum (DQ) signal function, I_{nDQ}, that has the advantage of being independent of any temperature-dependent true relaxation (decay) effect. It is dominated by the dipolar interactions and independent of the polymer dynamics. For this purpose, the directly measured experimental DQ build-up curve (I_{DQ}) must be relaxation-corrected by the use of the also measured reference intensity (I_{ref}). Initially, I_{ref} contains a signal from not only the dipolar-coupled network chains but also the uncoupled, isotropically mobile components such as sol, dangling chains, and so on. The total MQ magnetization ($I_{\Sigma MQ}$) needed for normalization is the sum of I_{DQ} and I_{ref} but only after subtracting the non-network contributions. This fraction has a slower relaxation and can be easily identified (Figure 1a). In the studied hydrogels, even though we used deuterated water to dissolve the polymer, we found a non-negligible water signal resulting from actual residual water and exchanged −OH protons. Therefore, we had to identify and subtract two exponential long-time contributions to $I_{\Sigma MQ}$ (i.e., the noncoupled fraction of polymer chains (B fraction in eq 2) and the solvent signal (fraction C)), which relax with longer relaxation times ($T_{2C}^* \gg T_{2B}^*$)

$$I_{\Sigma MQ} = I_{DQ} + I_{ref} - B\,e^{-2\tau_{DQ}/T_{2B}^*} - C\,e^{-2\tau_{DQ}/T_{2C}^*} \quad (2)$$

This corrected quantity is used to normalize the DQ intensity. (See Figure 1b.)

$$I_{nDQ} = I_{DQ}/I_{\Sigma MQ} \quad (3)$$

Finally, it is important to point out that in rubber networks the distribution effects of D_{res} (related to different end-to-end separations and polydispersities of network chains) usually do not play any role.[56] Therefore, the normalized DQ build-up curve of a bulk rubber can be analyzed in the quasi-static limit in terms of a single D_{res}[38]

$$I_{nDQ}(\tau_{DQ}, D_{res}) = \frac{1}{2}\left(1 - \exp\left[-\frac{2}{5}D_{res}^2\tau_{DQ}^2\right]\right) \quad (4)$$

However, the complex and heterogeneous PVA network structure,[28,31] in addition to specific effects related to the swollen state of the sample (which is proven to be heterogeneous in polymer networks[57]), leads to large deviations from the inverted Gaussian shape in the studied PVA gels. The actual coupling distribution (related to a microstructurally heterogeneous distribution of constraints) can be evaluated by using fast Tikhonov regularization of the experimental data.[40,58−60] The insert in Figure 1b shows the broad distribution of dipolar interactions in PVA networks. It resembles a gamma distribution and is consistent with observations of very heterogeneous network structures proposed in the literature.[28,31] All analyzed samples showed a similar distribution shape independently of the number of freezing−thawing cycles.

Because regularization analysis is subject to some limitations[42] (further work about this point is in progress), we have analyzed all build-up curves under the assumption of the gamma distribution of dipolar couplings that is predicted by the Gaussian distribution of end-to-end separations (but which is screened in bulk elastomers)[38,42]

$$I_{nDQ}(\tau_{DQ}, D_{avg}) = \int_0^\infty \frac{1}{2}\left(1 - \exp\left[-\frac{2}{5}D_{res}^2\tau_{DQ}^2\right]\right) \times \frac{2}{\sqrt{\pi}}\sqrt{\frac{27D_{res}}{8D_{avg}^3}}\,e^{-3D_{res}/(2D_{avg})}\,dD_{res} \quad (5)$$

Upon fitting, the integral is numerically evaluated within the curve fitting environment of the Origin software. In using this distribution, we do not want to imply that this distribution is of any significance in the studied structure; the resulting build-up curves merely describe all of our experimental build-up data very well and have the benefit of not introducing an additional fit parameter, yet they provide a well-defined average residual coupling D_{avg}. (The width of the gamma distribution is directly related to the average.)

Finally, note that the MQ analysis pertains to the mobile fraction of the cryogels only; this fraction always constitutes the major part of the sample (>80%); the rest is rigid crystallites, and the signal of which rapidly relaxes and is not observable under the conditions of the MQ experiment.

Pulsed Mixed Magic-Sandwich Echo. According to previous papers, polymer crystallites act as junctions in PVA networks obtained by freezing−thawing cycles.[28,29,31,34] Solid-state NMR is a useful method for characterizing polymer crystallinity or phase composition in this type of system. The main concept is that the crystalline signal usually decays in the first 20 μs of the free-induction decay; therefore, the signal detected after the dead time (12 μs in our case) partially conceals this information. Nevertheless, in some works, the fraction of protons in a glassy state in PVA gels was estimated by monitoring the FID intensity during the first 20 μs,[61−63] which renders these studies qualitative. Different solutions were reported in the literature. Perhaps the most important

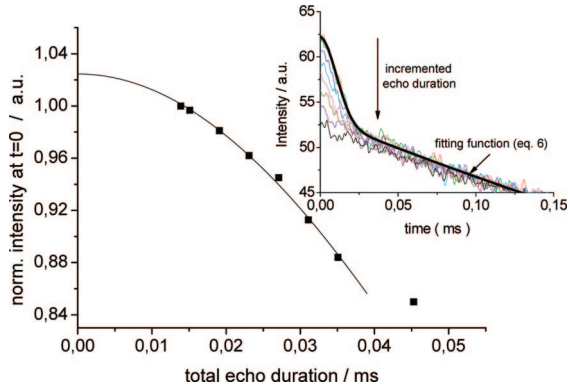

Figure 2. Parabolic (Gaussian) extrapolation of the maximum MSE-refocused FID intensities to $t = 0$. It indicates only minor losses of rigid signal at the shortest echo time (10% on a scale relative to the total crystallinity). The inserted graph shows MSE-refocused FIDs of 10% PVA gel after six cycles measured at different echo times at room temperature (304 K).

is the use of solid echoes with different echo delays combined with back extrapolation[64] to correct for its inability to refocus the dipolar interactions in a multiple-spin system fully. Certainly, the best approach is the use of a spectrometer with short (1 to 2 μs) dead time.[65]

The use of an MSE was recently proposed[44] as a more effective method for refocusing the multiple dipolar interactions that lead to the fast decay of the initial part of the FID, therefore removing the dead-time problem and obtaining a near-quantitative rigid fraction determination in polymer systems. Under the same experimental conditions, differences of ~40% in the quantity of rigid phase in PVA compounds were observed comparing FIDs and MSE-refocused FIDs (data not shown). Figure 2 shows the MSE-FIDs for different total echo duration (realized by increasing the interpulse spacings). The signal decay data are well represented by a Gaussian function (parabolic initial decay), and its extrapolation to $t = 0$ allows us to conclude that the signal loss is negligible. (It could be estimated to be ~2% on the absolute scale, which corresponds to 10% on the relative scale.)

However, note that even for the MSE the refocusing efficiency breaks when there is molecular motion on its time scale. In particular, this may be the case if the observed rigid component is glassy rather than crystalline and close to T_g. Under any condition irrespective of temperature, however, the typical decay time upon incrementing the echo was never significantly shorter than the (relatively weak) decay seen in Figure 2, which is ultimately associated with the breakdown of the pulse sequence efficiency because of higher-order imperfections. We thus conclude that all observed rigid signals are associated with crystal-like domains; otherwise, a significant signal loss upon going through T_g would have been observed.

Therefore, MSE-FID curves were used to quantify the fraction of fast-decaying rigid polymer present in PVA gels. The first fast decay (caused by the rigid polymer fraction) in the MSE-FIDs (insert in Figure 2) has a quasi-Gaussian decay, whereas the slower signal decay could be fitted with an exponential function. Therefore, the first 140 μs of the normalized MSE-FID curves (unity signal for zero time) were fit according to eq 6

$$I_{\mathrm{MSE-FID}} = A\exp\left(-\left(\frac{\tau}{T_{2\mathrm{hard}}}\right)^{b}\right) + (1-A)\exp\left(-\frac{\tau}{T_{2\mathrm{soft}}}\right) \quad (6)$$

In this expression, A is the fraction of detectable rigid phase in the sample and b is an adjustable parameter for a better fit of the fast decay shape. In all of the cases, $b \approx 2$ (i.e., the crystalline fraction is described by a Gaussian function). In addition, to reference the hard polymer phase to the total amount of polymer (instead of the sample fraction), we corrected the A parameter according to the actual fraction of polymer in the sample obtained from saturation recovery experiments (note again that the samples contain residual water) on the basis of the fact that water has a much longer T_1 relaxation time. From such experiments, and assuming no significant NOE transfer between the species on the same time scale, the water content can be obtained from a biexponential fit

$$M_z = D\left(1-\exp\left(-\frac{\tau}{T_{1\mathrm{W}}}\right)\right) + (1-D)\left(1-\exp\left(-\frac{\tau}{T_{1\mathrm{P}}}\right)\right) \quad (7)$$

where D is the water fraction in the sample and T_{1W} and T_{1P} are the longitudinal relaxation time constant of water and polymer, respectively (with $T_{1W} \geqslant T_{1P}$). For example, at $T = 304$ K, the relaxation times were $T_{1W} = 1520$ ms and $T_{1P} = 60$ ms for a network with 10% PVA after seven freezing−thawing cycles. The fast-decaying rigid crystallite signal was not detected in these experiments (the FID was evaluated at a time beyond 50 μs) such that D is determined relative to the mobile polymer fraction (i.e., $(1 - A)$ in eq 6).

Finally, the rigid polymer fraction discussed below was obtained according to

$$\text{rigid polymer fraction (\%)} = \frac{A}{(1-D)}100 \quad (8)$$

Obviously, for these corrections, it is essential to use a recycle delay that is long enough to observe the full equilibrium magnetization of the sample ($5(T_{1W})$ was used as a recycle delay in all experiments, i.e., ~7−20 s depending on the temperature).

Results and Discussion

The aim of this work is to study the structure and phase composition of PVA cryo-gels by using a low-field NMR spectrometer. To revise the structural models suggested in the literature, we will separately analyze the effects of three factors on the PVA network structure: (i) the number of applied freezing−thawing cycles, (ii) the temperature and melting process, and (iii) the aging process. To achieve this objective, in every point, DQ experiments were performed to quantify the proportion of noncoupled network defects, and the molecular weight between cross-links and MSE-FID pulse sequence were applied to determine the rigid fraction of the polymer.

Effect of Freezing−Thawing Cycles. The starting point of our study is the characterization of two isotropic solutions of 10 and 20% (w/v) of PVA in water. The 10% PVA solution does not give any detectable DQ signal, but for the decay (I_{ref}) data, two different processes can be identified (i.e., the decay of the polymer magnetization and the water relaxation). This result demonstrates that under these preparation and measurement conditions, the dilute solution can be considered to be nonentangled and above the gelation threshold. This is not a trivial result because DQ experiments are, in principle, sensitive to transient links (entanglements or hydrogen bonds), and this indeed appears indicated by the 20% PVA solution; under the same preparation conditions, DQ experiments did yield a detectable build-up curve. However, this is in our case due to a nondissolved or partially gelled PVA subphase. To avoid this problem, 20% PVA solutions were prepared under more vigorous stirring as well as higher temperatures up to 90 °C. In this way, a totally isotropic solution of polymer was obtained according the DQ experiments.

DQ experiments were performed on PVA samples subject to different numbers of freezing−thawing cycles to determine the evolution of noncoupled network defects as well as the network mesh size. In Figure 3, we can see that after the first freezing−thawing cycle, ~50% of the polymer chains are coupled and are therefore part of the network, whereas the rest are not linked to it or at least belong to elastically inactive dangling chains or loops. The number of PVA chains incorporated in the gel network increases with the successive cycles

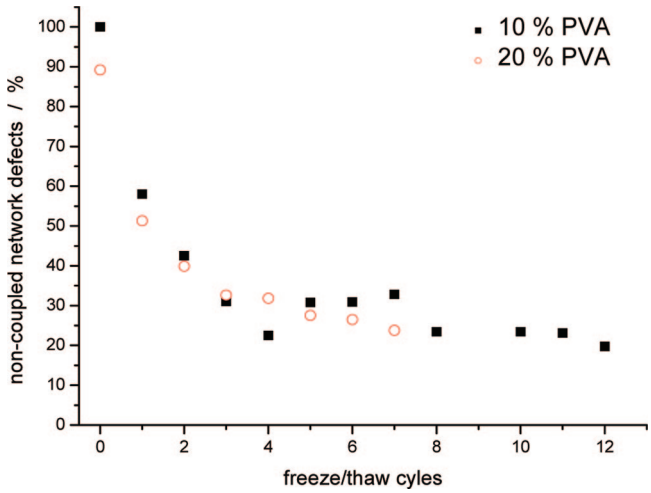

Figure 3. Variation of noncoupled network defects (i.e., non-cross-linked polymer chains, dangling chains, and loops) as a function of the number of freezing−thawing cycles for the studied PVA solutions.

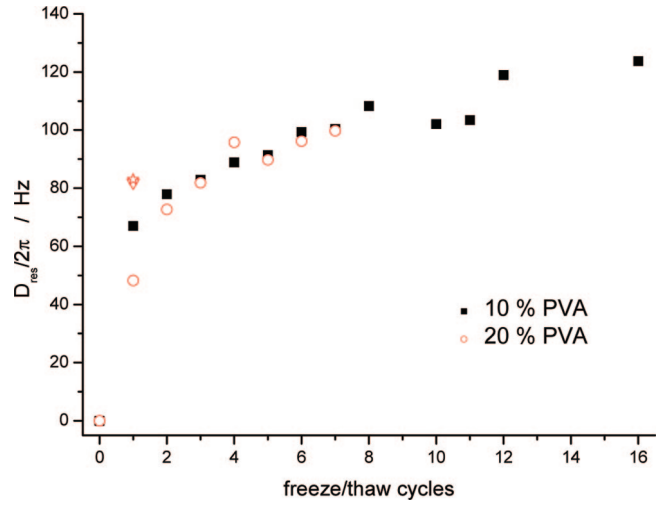

Figure 4. Variation of the average residual dipolar couplings (directly related to $1/N$ and therefore the cross-link density or the inverse mesh size) extracted from DQ experiments as a function of the number of freezing−thawing cycles for the studied PVA solutions. ▽ represents a sample containing 20% PVA after 3 h of freezing, and ☆ is from the same sample after 16 h of freezing.

until it reaches a plateau after the sixth cycle, where the network has the minimum defect content. This important result shows that independent of the number of freezing−thawing cycles applied to a PVA solution ∼25% of the polymer is not coupled and therefore should not be elastically active. This is a very significant observation that is usually not taken into consideration when mechanical,[14,30] dynamic-mechanical,[9−30] or rheological[18,27] properties of this material are analyzed. Urushizaki et al.[66] have related the viscoelastic properties of this type of gel to the nonincorporated PVA chains, and they have estimated their amount from the difference in weight between the polymer gel before and after immersion in distilled water. They found that ∼10% of the polymer was not incorporated after the first freezing−thawing cycle. Similar results were also indirectly inferred from the measure of intradiffusion coefficients of micellar aggregates of surfactant molecules dissolved in these types of gels.[67] Obviously, our experimental values are much larger because we detect not only the non-cross-linked chains but also the dangling chains and other nonelastic network defects (e.g., loops). The effect of D_2O in measured noncoupled network defects is another important point to take into consideration when this fraction of polymer is analyzed. PVA monomers have an exchangeable proton (−OH), which, in presence of D_2O, could be replaced by deuterium that is undetectable by ^{1}H NMR, whereas the proton will become detectable as water (HDO). Free water signal (H_2O or HDO) is subtracted from the long-time decay of the signal because it can be identified by its own longer T_2. However, the number of noncoupled network defects could be slightly overestimated because of the proton−deuterium exchange.

In addition, the decrease in the number of defects is correlated with an increase in D_{res} that is proportional to the network chain order parameter (eq 1), see Figure 4. The formation of cross-links (independent of their nature) renders the polymer segmental motion nonisotropic, whereby the chain segments become ordered with respect to the end-to-end distance, and residual dipolar couplings arise. According to this basic principle, the increase in D_{res} is directly related to the (inverse) length of the chains between the constraints. Similar to the observation for the noncoupled network defects, the network chain length appears to approach a plateau after cycle number six, yet the tendency is not as clear as the former result. Even after 16 cycles, the cross-link density still appears to increase.

With this observation, it is important to note that samples with different polymer concentration appear to exhibit the same behavior during gelation. A possible explanation could be that in the framework of a heterogeneous scenario cross-linking occurs via partial crystallization in the nonfrozen parts of the sample; it simply means that in less concentrated samples more water freezes. This fact could explain the dependence of the dimension and shape of pores on polymer concentration and the regimes of cryogenic treatment.[20] In this context, it appears to be worthwhile to study the influence of the actual freezing temperature, which should affect the polymer concentration under the conditions at which the crystallites are formed.

However, the freezing time (especially in the first cycle when the network is formed) seems to have some influence in the gel network structure. As is shown in Figure 4, the apparent dipolar coupling constant is very low (∼48 Hz) after 1 h of freezing at −32 °C. If the freezing period is increased to 3 h, then the cross-link density of the gel almost doubles (∼82 Hz), whereas longer freezing (e.g., 16 h) does not lead to further variation. This may indicate that 1 h of freezing is not long enough to complete the process, and for this reason, further analyses are based on samples with a first freezing cycle of 12 h and subsequent cycles of 3 h each.

Returning to the origin of the PVA networks produced via freezing−thawing cycles from homogeneous polymer solutions in water, it appears to be well demonstrated by now that during the first freezing cycle, freezing of some water[32] increases the concentration of PVA in the still unfrozen phase.[31] Crystallization of PVA takes place in this concentrated microphase,[68] but it is kinetically frustrated by the gelation of the polymer solution.[28,31,32] This fact could explain the small size of these primary crystallites (∼5 nm),[28,29,31] which then act as physical junctions between the amorphous and mobile polymer chains. Results extracted from the MSE-FID curves of the PVA gels after the first freezing−thawing cycle (Figure 5) indicate that ∼8% of the polymer behaves like a rigid solid. This rigid fraction increases with the number of cycles until it reaches a plateau close to cycle number six, just as our other reported network properties. The maximum amount of rigid phase estimated by our NMR methodology (∼20% of the total polymer) is substantially higher than the crystallinity of similar samples deduced by DSC[27,28] as well as some other ^{1}H NMR methods.[18,28]

In all cases, the crystallinity of PVA cryo-gels obtained in DSC studies is estimated to be ∼5% (not taking into account

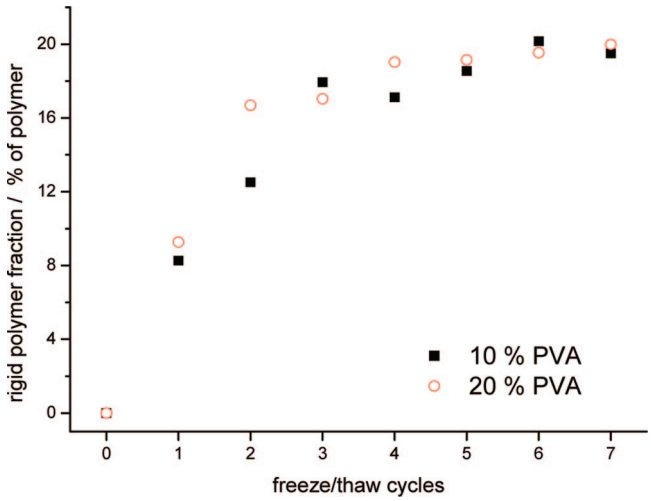

Figure 5. Variation of the rigid (crystalline) polymer fraction extracted from MSE-FID curves as a function of the number of freezing−thawing cycles for the studied PVA solutions.

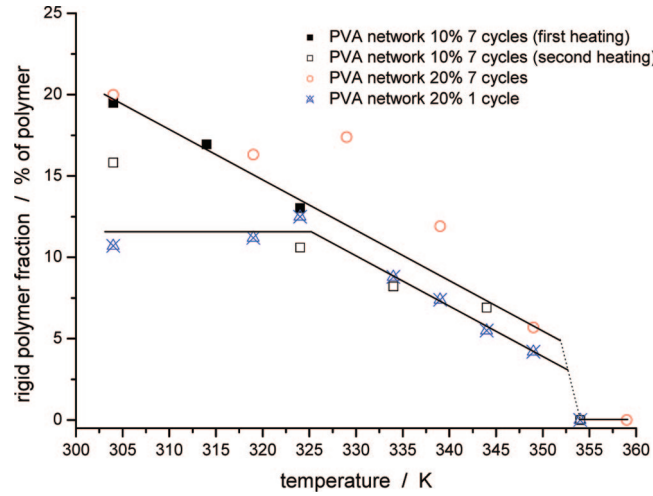

Figure 6. Variation of the rigid polymer fraction (extracted from MSE-FID experiments) as a function of temperature for PVA gels formed after seven freezing−thawing cycles. A network with 10% PVA was first heated until 324 K (■) and then kept at room temperature for 12 h before the second heating procedure was performed (□). A solution with 20% PVA was submitted to two different treatments, that is, one freezing−thawing cycle and seven freezing−thawing cycles, respectively. Lines are only to guide the eye. All samples were frozen for 12 h in the first cycle and 3 h in the subsequent cycles.

studies of dry networks[34] because the structure should be different). However, as was pointed out by Willcox et al.,[28] this magnitude could very well be underestimated because the heat of fusion of the crystals in gels may be substantially lower than the assumed PVA bulk value because of their small size and large surface effects (hydrogen bonds to surrounding water, etc.). In addition, another important point is the difficulty in measuring small quantities of crystal phase in dilute gels via calorimetric methods in general; for example, a crystallinity of 8% in a gel with a PVA concentration of 20% represents only a sample fraction of 0.016. Nevertheless, this difficulty seems to be reduced by the use of microcalorimetry. In this way, similar results were obtained by performing this type of measurement on gels with low PVA concentrations,[8] although the uncertainties related to the obtained results are still large.

For these reasons, the use of solid-state NMR seems to be a better methodology for quantifying the crystallinity in dilute PVA gels. However, there are still some discrepancies in the total amount of rigid phase measured by the use of different NMR methodologies. Ricciardi et al.[18] estimated the crystallinity of PVA gels after 11 freezing−thawing cycles to be ∼8% by analyzing the first microsecond of the ^{1}H FID. Clearly, as was pointed out in the Experimental Section, this experimental procedure falls victim to the dead-time problem. Depending on the spectrometer, the amount of rigid signal lost during this time could be more or less significant. (Ref 15 does not specify the dead time; therefore, it is not possible to estimate the related error.) For example, our low-field spectrometer has a dead time of ∼12 μs; therefore, the FID analysis would lead to an underestimation of the rigid polymer fraction by ∼50%. By using different ^{13}C NMR experiments (direct polarization as well as ^{1}H−^{13}C cross polarization), Willcox et al.[28] established that after the first freezing−thawing cycle, PVA gel contains a rigid polymer phase of ∼5 ± 2%, increasing up to 12 ± 4% after cycle number 12. These last values are closer to our experimental estimation but are still far away. As was pointed out by the authors,[28] the relative fraction comparing different samples could be estimated with a high accuracy, but the used methodology (in particular, the use of the intrinsically nonquantitative cross polarization) does not give a reliable absolute crystallinity.

In conclusion, the key to obtaining the most accurate crystal fraction in these dilute polymer samples is to use a solid-state NMR method that allows us to detect the rigid part fully by refocusing the multispin dipolar interactions with the MSE, thus solving the dead-time problem and minimizing the signal loss. Of course, detecting the more-sensitive and 100% abundant protons instead of the naturally abundant ^{13}C is an additional advantage, which more than compensates for the use of an intrinsically less-sensitive low-field spectrometer.

Summarizing all results discussed so far, the network structure of PVA cryo-gels is very apparently based on the formation of rigid polymer areas (most probably polymer crystallites) during the cooling process. After the first cycle, almost half (∼8%) of the final amount (20%) of the rigid phase is already formed. In this stage, ∼50% of all polymer segments are part of the network structure. Subsequent freezing−thawing cycles increase the rigid polymer fraction, which has two consequences: First, the noncoupled polymer fraction is further reduced (i.e., more PVA segments become elastically active), and second, the network mesh size is further reduced but only slightly during further freezing−thawing cycles. Therefore, we believe that subsequent freezing−thawing cycles not only increase the size of the crystals formed during the first freezing process but also lead to the creation of other more imperfect crystals.

Temperature Effect: Melting Process. Independent of the polymer concentration of the gel, the melting of smaller and more imperfect secondary crystals takes place at lower temperature and over a large range, leading to a continuous decrease in the detected rigid polymer phase with the temperature (Figure 6). At ∼75−80 °C (in good agreement with the main endotherm observed in DSC measurements[27−29]), this quantity drops below the detection limit. This should be correlated with the melting of the main (primary) crystals (estimated to ∼5% of the polymer fraction) that support the network structure of the gel. These results are consistent with DSC measurements[27,28] because they show an increase in the melting endotherm that corresponds to the initial crystals as well as to the appearance of a second endotherm at lower temperatures when the number of freezing−thawing cycles was increased for a given PVA solution.

The effect of the number of freezing−thawing cycles on the crystallinity is easily understandable by comparing the evolution of the rigid polymer fraction of a PVA gel obtained after seven cycles with that of a PVA gel after only one freezing−thawing cycle (Figure 6). The onset of melting after only one freezing cycle is estimated to be ∼50 °C, leaving the rigid polymer

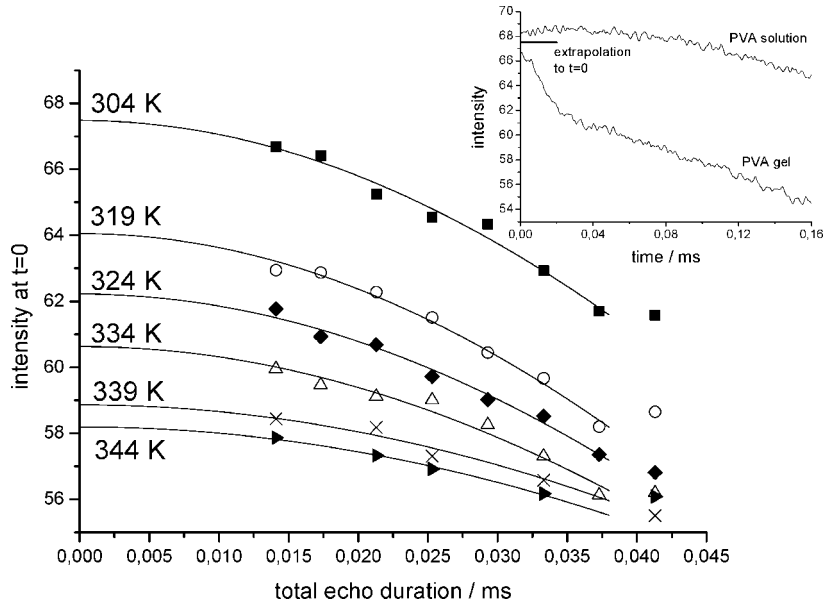

Figure 7. Variation of the initial signal intensity of MSE-FIDs with increasing echo delay at different temperatures for a PVA gel containing 20% polymer after one freezing−thawing cycle (12 h of freezing and 1 h thawing). Lines are the result of parabolic fits. The insert presents the MSE-FID of the PVA gel measured at 304 K with the minimum echo delay (0.0022 ms) as well as the estimated intensity at zero echo time in comparison with the MSE-FID of the isotropic solution of the same sample measured under the same conditions after complete melting at 90 °C.

fraction constant at lower temperatures. Therefore, subsequent cycles seem to create more, yet imperfect, secondary crystallite structures. Above 50 °C, all samples exhibit a similar behavior related to the partial melting of primary crystals or to the melting of less-perfect secondary structures. Importantly, the temperature above which it is not possible to detect any more signal of rigid polymer remains invariant, yet the final fraction seems to increase slightly with the number of cycles. Therefore, according to this result, freezing−thawing cycles have a direct influence on not only the number of crystals formed during the first freezing process but also the creation of other more imperfect secondary crystallites.

To ensure that the results shown in Figure 6 are not artifacts produced by different magnetization relaxation at different temperatures that could possibly arise from regions that undergo a glass-to-liquid rather than a melting transition, the evolution of the signal at any given temperature was studied as a function of echo delay, see Figure 7. At all of the measured temperatures, similar behavior was found, with a loss of intensity estimated to between 0.7 and 1.8% for the two extreme cases, which corresponds to a constant 10% loss on a relative scale, as is usually found. Importantly, the drop in overall signal corresponds, within the error margins, to the expected drop due to the Curie factor (temperature-dependent spin polarization). In addition, a direct check is the control of the total intensity, comparing the PVA gels to the corresponding PVA solutions (insert in Figure 7). It is seen that no significant signal is lost/undetectable (we observe almost all protons in the sample), and from this, it is clear that the loss of intensity caused by the MSE in PVA gels is at a minimum, with no other (hidden) phenomena that could be related to an intermediately mobile (almost glassy) rigid fraction. Given this experimental evidence, the decay of the rigid ^{1}H fraction with temperature can be related to only a melting of PVA crystallites.

Obviously, the temperature-dependent variation of the rigid polymer phase has a direct effect on the network structure, as shown in Figure 8. The melting of secondary crystals leads to an almost exponential increase in the number of network defects (obviously, in a reversible pathway, comparing the phenomenon with the effect of successive freezing−thawing cycles). However, the network mesh size (as measured by the residual dipolar coupling) remains almost constant. This means that secondary crystallization is very important in the network organization, reducing the number of network defects and therefore increasing the number of polymer segments that are elastically active. However, the molecular weight between the constraints appears to be dictated mostly by the primary crystallites formed during the first freezing cycles. For this reason, the network is completely destroyed at temperatures of ∼80 °C when the primary crystal phase is molten, leaving no observable DQ signal (i.e., an isotropic PVA solution is formed). On the side, we note that the differences in the D_{avg} values given in Figures 4 and 8b, which indicate a 50% decreased mesh size for the samples studied in Figure 8, are related to the increase in the freezing time (12 h in the first step and 3 h in the successive cycles instead of 1 h) used in each cycle, as pointed out above.

These NMR results on the mesh size perfectly agree with the trends observed in studies of mechanical properties reported in the literature. Clearly, the elastic behavior of PVA gels depends on the number of freezing−thawing cycles.[9,18,30,66] The crystallinity increases, whereas the mesh size is only slightly reduced. Therefore, the main factor that determines the improvement of the mechanical properties upon further cycles should be associated with the number of elastically active chains. The polymer concentration in the original aqueous solution has an important effect on the elastic properties;[9,18] that is, the elastic modulus increases. However, in the view of our data, this does not appear to have important consequences for the actual network structure; that is, there are no large variations in the network mesh size. Therefore, the reported variations are simply related to differences in polymer concentration. In addition, different works[9,66] demonstrate a slight decrease in the elastic modulus with the temperature, until a major drop occurs at 50 °C.[65] This is obviously related to the partial melting of secondary and more imperfect crystallites that leads to an increasing amount of network defects (elastically inactive chains). At temperatures close to 80 °C, the complete loss of crystallinity essentially liberates all chains, and the system drops below the gel point. In view of the important role of the substantial polymer amount that is not elastically active (free and dangling chains, loops), it may be worthwhile to reconsider detailed frequency-dependent mechanical measurements, where these

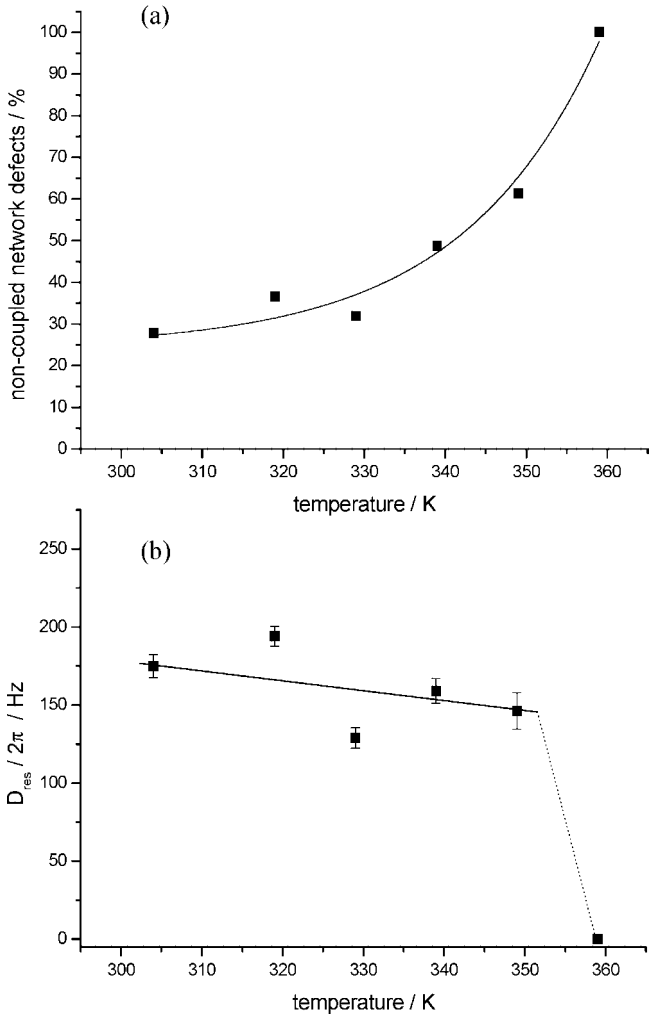

Figure 8. Variation of (a) the network defect fraction and (b) the inverse mesh size (given by D_{avg} measured by MQ NMR) with temperature for the 20% PVA gel prepared after seven freezing−thawing cycles (12 h first freezing cycle, 3 h subsequent cycles). Error bars represent the fitting uncertainty, whereas lines are only guides to the eye.

components should contribute to an increased loss modulus over the frequency range covering their relaxation.

The capacity of our investigated systems to be transformed from an isotropic aqueous solution to a physical cryo-gel by the application of freezing−thawing cycles, including thermal reversibility back to an isotropic PVA solution, is in clear contradiction with the assertion that covalent bonds could form between the polymer chains during gelation.[8,33] If covalent cross-links were an important contribution to the final gel properties, then residual couplings should persist even above the melting temperature of the crystallites, which is not the case. However, the presence of (rapidly tumbling) microgels above the main melting point cannot be ruled out and is in fact indicated by the relatively high viscosity (as checked by a simple tilt test). However, we point out that even the pristine 20% PVA solution exhibited some detectable DQ signal, indicating extended gel-like structures, unless it was heated to >90 °C. Therefore, an undetectably small fraction of crystallites (or extended hydrogen-bonded aggregates) may always be present, even at >80 °C, and hold the system close to the gel point, depending on the sample and its thermal history. From our perspective, permanent bonds can be ruled out as a major factor determining the cryo-gel structure.

Aging Effect. Finally, we address aging phenomena that are a part of the data shown in Figure 6 and were not commented on until now. After heating a sample containing 10% PVA to 50 °C and recording the loss of crystallinity, the sample was stored for 12 h, and another measurement was performed at room temperature. The amount of rigid polymer fraction after 12 h of storage was again considerably increased, as can be seen in Figure 6. Yet, this new crystalline fraction melts at rather low temperatures, which again indicates the growth of secondary crystallites. Similar prominent aging effects have been reported in the literature.[4,9,28−30]

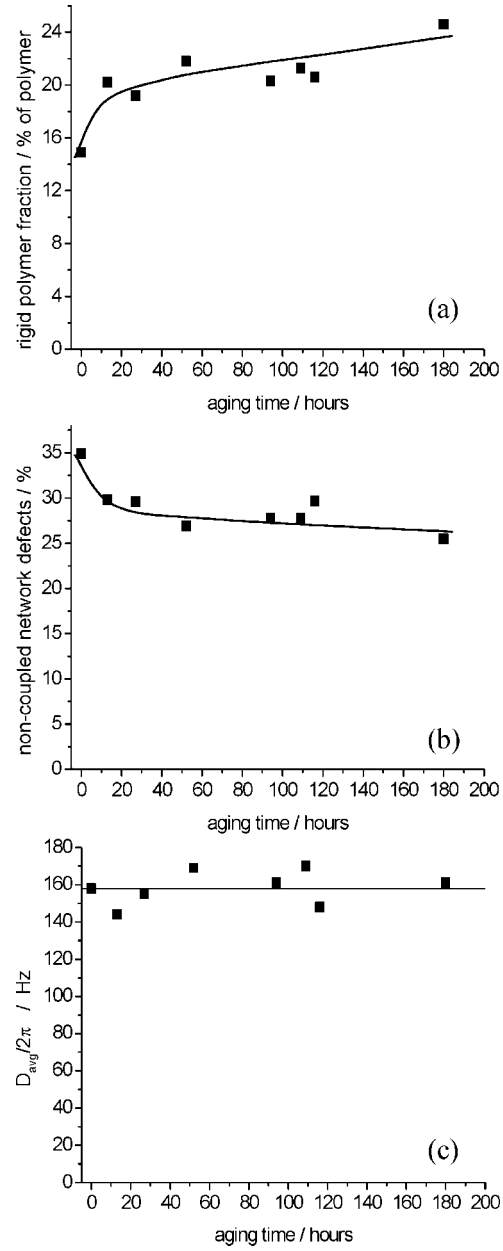

Figure 9. Effect of aging on (a) the rigid polymer fraction, (b) the noncoupled defects fraction, and (c) the average residual dipolar coupling of a gel with 10% PVA obtained after seven freezing−thawing cycles (12 h of freezing for the first cycle and 3 h for the following cycles). All properties were measured at 30 °C. Lines are only guides to the eye.

For more clear evidence, a sealed sample containing 20% PVA was submitted to seven freezing−thawing cycles (with 12 h of freezing in the first cycle) and was characterized after different storage times at room temperature. According to Figure 9, aging clearly increases the secondary population of imperfect crystals. It also increases the amount of elastically active polymer segments but has no significant effect on the network

mesh size. Therefore, aging effects on PVA gel properties[4,9,28−30] are again mainly related to an increasing fraction of polymer incorporated into the network structure and not to a decrease in mesh size.

Conclusions

PVA hydrogels obtained by freezing−thawing cycles exhibit a complex heterogeneous network structure. This physical gel is supported by rigid polymer areas (PVA crystallites) that act as junctions between the remaining mobile and entropically elastic polymer chains and thus determine the network mesh size. In our study, the crystallites are quantitatively detected as a rigidlike fraction of quickly relaxing (and fully refocused to overcome the dead-time problem) magnetization, and the mesh size is deduced from MQ experiments that measure residual dipolar couplings, the latter arising from constraints on the motion of the mobile chains (i.e., cross-links) that render the segmental motion locally anisotropic.

The most important crystal fraction forms in the first freezing cycle, and subsequent freezing−thawing cycles produce only a slight increase in the initial crystal size as well as induce the formation of more imperfect, secondary crystallites. This secondary crystal fraction (which constitutes around two-thirds of the total crystal phase in samples submitted to a large number of cycles, extended aging, or both) plays an important role by increasing the number of elastically active polymer chains, but it does not appreciably affect the mesh size. This effect also diminishes when longer freezing cycles are applied.

PVA cryo-hydrogels are shown to be totally thermoreversible; that is, PVA physical networks can be transformed into an isotropic aqueous solution by increasing the temperature. During this process, the more imperfect crystals are molten first, and the number of network defects increases exponentially. In contrast, the network mesh size does not undergo significant variations until the primary crystal phase is molten at temperatures of ∼80 °C. Our experiments did not reveal any evidence of the possible formation of covalent cross-links between PVA chains during gelation; no residual couplings were detected after the melting of this primary crystal fraction.

Independent of the number of cycles, the aging, or the polymer concentration in the original PVA solution, a considerable fraction of polymer (at least 25%) is not elastically active, which is a result that is not yet not taken into account in the large body of literature addressing the formation and the properties of PVA cryo-hydrogels. This finding is central to the interpretation and understanding of the elastic properties of this useful material and must be taken into account in a reinterpretation of the origin of the changes of the elastic moduli of PVA cryogels.

Finally, it is important that the in-depth study of both processes (i.e., the PVA gelation by the application of freezing−thawing cycles) as well as the destruction of the network structure by heating were, for the first time, entirely based on the use of an inexpensive low-field solid-state NMR spectrometer. We show that the combination of different advanced NMR strategies, that is, MQ spectroscopy and component analysis of MSE-refocused free-induction decays, is vital for obtaining quantitative information on network structure and phase composition (crystallinity), respectively, to arrive at conclusions that can be matched with information extracted from other diverse techniques.

In addition, the use of low-field solid-state NMR spectroscopy not only is useful for extracting structural information but also could be a powerful tool for investigating the polymer dynamics of these complex systems.

Acknowledgment. J.L.V. thanks the Alexander von Humboldt Foundation as well as the Ministerio de Educacion y Ciencia (Spain) for his fellowships. K.S. acknowledges financial support by the Deutsche Forschungsgemeinschaft (DFG, SFB 418, and SA982/1-2). Financial support from CICYT (MAT 2008-1073) is also gratefully acknowledged.

References and Notes

(1) Schmedlen, K. H.; Masters, K. S.; West, J. L. *Biomaterials* **2002**, *23*, 4325–4332.
(2) Doria-Serrano, M. C.; Ruiz-Trevino, F. A.; Rios-Arciga, C.; Hernandez-Esparza, M.; Santiago, P. *Biomacromolecules* **2001**, *2*, 568–574.
(3) Hassan, C. M.; Stewart, J. E.; Peppas, N. A. *Eur. J. Pharm. Biopharm.* **2000**, *49*, 161–165.
(4) Hassan, C. M.; Peppas, N. A. *Adv. Polym. Sci.* **2000**, *153*, 37–65.
(5) *Thermoreversible Gelation of Polymers and Biopolymers*; Guenet, J. M., Ed.; Academic Press;: New York, 1992.
(6) Nijenhuis, K. T. *Adv. Polym. Sci.* **1997**, *130*, 1–12.
(7) Peppas, N. A. *Makromol. Chem.* **1975**, *176*, 3433–3440.
(8) Hernandez, R.; Lopez, D.; Mijangos, C.; Guenet, J. M. *Polymer* **2002**, *43*, 5661–5663.
(9) Hernandez, R.; Sarafian, A.; Lopez, D.; Mijangos, C. *Polymer* **2004**, *46*, 5543–5549.
(10) Hernandez, R.; Rusa, M.; Rusa, C. C.; Lopez, D.; Mijangos, C.; Tonelli, A. E. *Macromolecules* **2004**, *37*, 9620–9625.
(11) Pines, E.; Prins, W. *Macromolecules* **1973**, *6*, 888–895.
(12) Feke, G. T.; Prins, W. *Macromolecules* **1974**, *7*, 527–530.
(13) Komatsu, M.; Inoue, T.; Miyasaka, K. *J. Polym. Sci., Part B: Polym. Phys.* **1986**, *24*, 303–311.
(14) Stauffer, S. R.; Peppas, N. A. *Polymer* **1992**, *33*, 3932–3936.
(15) Hickey, A. S.; Peppas, N. A. *J. Membr. Sci.* **1995**, *107*, 229–237.
(16) Peppas, N. A.; Scott, J. E. *J. Controlled Release* **1992**, *18*, 95–100.
(17) Ricciardi, R.; Auriemma, F.; de Rosa, C. *Macromol. Symp.* **2005**, *222*, 49–63.
(18) Ricciardi, R.; Gaillet, C.; Ducouret, G.; Lafuma, F.; Lauprete, F. *Polymer* **2003**, *44*, 3375–3380.
(19) Lozinsky, V. I.; Plieva, F. M. *Enzyme Microb. Technol.* **1998**, *23*, 227–242.
(20) Lozinsky, V. I.; Galaev, I. Y.; Plieva, F. M.; Savinal, I. N.; Jungvid, H.; Mattiasson, B. *Trends Biotechnol.* **2003**, *21*, 445–451.
(21) Lozinsky, V. I.; Solodova, E. V.; Zubov, A. L.; Simenel, I. A. *J. Appl. Polym. Sci.* **1995**, *58*, 171–177.
(22) Lozinsky, V. I.; Damshkaln, L. G.; Shaskol'skii, B. L.; Bubushkina, T. A.; Kurochkin, I. N.; Kurochkin, I. I. *Colloid J.* **2007**, *69*, 747–764.
(23) Lozinsky, V. I.; Damshkaln, L. G.; Kurochkin, I. N.; Kurochkin, I. I. *Colloid J.* **2008**, *70*, 189–198.
(24) Wu, W.; Shibayama, M.; Roy, S.; Kurokawa, H.; Coyne, L. D.; Noruma, S.; Stein, R. *Macromolecules* **1990**, *23*, 2245–2251.
(25) Kjoniksen, A. L.; Nyström, B. *Macromolecules* **1996**, *29*, 7116–7123.
(26) Yokoyama, F.; Masada, I.; Shimamura, K.; Ikawa, T.; Monobe, K. *Colloid Polym. Sci.* **1986**, *264*, 595–601.
(27) Watase, M.; Nishinari, K. *J. Polym. Sci., Polym. Phys. Ed.* **1985**, *23*, 1803–1811.
(28) Willcox, P. J.; Howie JR, D. W.; Schidt-Rohr, K.; Hoagland, D. A.; Gido, S. P.; Pudjijanto, S.; Kleiner, L. W.; Venkatraman, S. *J. Polym. Sci., Part B: Polym. Phys.* **1999**, *37*, 3438–3454.
(29) Ricciardi, R.; Auriemma, F.; de Rosa, C.; Laupretre, F. *Macromolecules* **2004**, *37*, 1921–1927.
(30) Ricciardi, R.; D'Errico, G.; Auriemma, F.; Ducouret, G.; Tedeschi, A. M.; de Rosa, C.; Laupretre, F.; Lafuma, F. *Macromolecules* **2005**, *38*, 6629–6639.
(31) Auriemma, F.; de Rosa, C.; Triolo, R. *Macromolecules* **2006**, *39*, 9429–9434.
(32) Auriemma, F.; de Rosa, C.; Ricciardi, R.; Lo Celso, F.; TRiolo, R.; Pipich, V. *J. Phys. Chem. B* **2008**, *112*, 816–823.
(33) Lozinsky, V. I.; Domotenko, L. V.; Vainerman, E. S.; Mamtsis, A. M.; Rogozhin, S. V. *Polym. Bull.* **1986**, *15*, 333–340.
(34) Hassan, C. M.; Peppas, N. A. *Macromolecules* **2000**, *33*, 2472–2479.
(35) Litvinov, V. M.; De, P. P. *Spectroscopy of Rubbers and Rubbery Materials*; Rapra: Shawbury, U.K., 2002.
(36) Simon, G.; Schneider, H. *Makromol. Chem., Macromol. Symp.* **1991**, *52*, 233–246.
(37) Demco, D. E.; Hafner, S.; Fülber, C.; Graf, R.; Spiess, H. W. *J. Chem. Phys.* **1996**, *105*, 11285–11296.
(38) Saalwächter, K. *Prog. Nucl. Magn. Reson. Spectrosc.* **2007**, *51*, 1–35.
(39) Graf, R.; Demco, D. E.; Hafner, S.; Spiess, H. W. *Solid State Nucl. Magn. Reson.* **1998**, *12*, 139–152.
(40) Schneider, M.; Gasper, L.; Demco, D. E.; Blümich, B. *J. Chem. Phys.* **1999**, *111*, 402–415.
(41) Saalwächter, K.; Gottlieb, M.; Liu, R.; Oppermann, W. *Macromolecules* **2007**, *40*, 1555–1561.

(42) Saalwächter, K.; Ziegler, P.; Spyckerelle, O.; Haidar, B.; Vidal, A.; Sommer, J. U. *J. Chem. Phys.* **2003**, *119*, 3468–3482.
(43) Saalwächter, K.; Heuer, A. *Macromolecules* **2006**, *39*, 3291–3303.
(44) Maus, A.; Hertlein, C.; Saalwächter, K. *Macromol. Chem. Phys.* **2006**, *207*, 1150–1158.
(45) Hedesiu, C.; Demco, D. E.; Kleppinger, R.; Buda, A. A.; Blumich, B.; Remerie, K.; Litvinov, V. M. *Polymer* **2007**, *48*, 763–777.
(46) Blumich, B.; Blumler, P.; Eidmann, G.; Guthausen, A.; Haken, R.; Schmitz, U.; Saito, K.; Zimmer, G. *Magn. Reson. Imaging* **1998**, *16*, 479–484.
(47) Cohen-Addad, J. P.; Vogin, R. *Phys. Rev. Lett.* **1974**, *33*, 940–943.
(48) Cohen-Addad, J. P. *Macromolecules* **1989**, *22*, 147–151.
(49) Cohen-Addad, J. P. *Prog. Nucl. Magn. Reson. Spectrosc.* **1993**, *25*, 1–316.
(50) Litvinov, V. M. *Macromolecules* **2006**, *39*, 8727–8741.
(51) Collignon, J.; Sillescu, H.; Spiess, H. W. *Colloid Polym. Sci.* **1981**, *259*, 220–226.
(52) Callaghan, P. T.; Samulski, E. T. *Macromolecules* **1997**, *30*, 113–122.
(53) Fischer, E.; Grinberg, F.; Kimmich, R.; Hafner, S. *J. Chem. Phys.* **1998**, *109*, 846–854.
(54) Graf, R.; Heuer, A.; Spiess, H. W. *Phys. Rev. Lett.* **1998**, *80*, 5738–5741.
(55) Saalwächter, K.; Herrero, B.; López-Manchado, M. A. *Macromolecules* **2005**, *38*, 9650–9660.
(56) Saalwächter, K.; Sommer, J.-U. *Macromol. Rapid Commun.* **2007**, *28*, 1455–1465.
(57) Saalwächter, K.; Kleinschmidt, F.; Sommer, J.-U. *Macromolecules* **2004**, *37*, 8556–8568.
(58) Weese, J. *Comput. Phys. Commun.* **1992**, *69*, 99–111.
(59) Weese, J. *Comput. Phys. Commun.* **1993**, *77*, 429–440.
(60) Roths, T.; Marth, M.; Weese, J.; Honerkamp, J. *Comput. Phys. Commun.* **2001**, *139*, 279–296.
(61) Feio, G.; Cohen-Addad, J. P. *J. Polym. Sci., Part B: Polym. Phys.* **1988**, *26*, 389–412.
(62) Feio, G.; Buntinx, G.; Cohen-Addad, J. P. *J. Polym. Sci., Part B: Polym. Phys.* **1989**, *27*, 1–24.
(63) Ebengou, R. H.; Cohen-Addad, J. P. *Polymer* **1994**, *35*, 2962–2969.
(64) Litvinov, V. M.; Penning, J. P. *Macromol. Chem. Phys.* **2004**, *205*, 1721–1734.
(65) Hansen, E. W.; Kristiansen, P. E.; Pedersen, B. *J. Phys. Chem. B* **1998**, *102*, 5444–5450.
(66) Urushizaki, F.; Yamaguchi, H.; Nakamura, K.; Numajiri, S.; Sugibayashi, K.; Morimoto, Y. *Int. J. Pharm.* **1990**, *58*, 135–142.
(67) Tedeschi, A.; Auriemma, F.; Ricciardi, R.; Mangiapia, G.; Trifuoggi, M.; Franco, L.; De Rosa, C.; Heenan, R. K.; Paduano, L.; D'Errico, G. *J. Phys. Chem. B* **2006**, *110*, 23031–23040.
(68) Ricciardi, R.; Mangiapia, G.; Lo Celso, F.; Padano, L.; Triolo, R.; Auriemma, F.; de Rosa, C.; Laupretre, F. *Chem. Mater.* **2005**, *17*, 1183–1189.

MA802172G